

VARIATION OF THE AXIAL AND RADIAL DIMENSIONS OF AN ELECTRON CLUSTER
DURING SYNCHROTRON ACCELERATION

F. A. KOROLEV, A. G. ERSHOV, and O. F. KULIKOV

Moscow State University

Submitted to JETP editor January 17, 1961

J. Exptl. Theoret. Phys. (U.S.S.R.) 40, 1644-1652 (June, 1961)

A high-speed moving film was made of a cluster of glowing electrons accelerated in the 660-Mev synchrotron of the Physics Institute of the Academy of Sciences. The law of variation of the axial and radial dimensions of the electron cluster was determined by measuring the film density. The results of the measurements are in good agreement with the theory in which radiative damping of the electron oscillations is taken into account. An increase of the radial dimensions of the cluster has been observed and can be explained by quantum effects in the electron radiation.

IN order to design large cyclic electron accelerators and accumulating systems, it is very important to know the law of variation of the axial and radial dimensions of the accelerated electron cluster. The axial, radial, and azimuthal dimensions of the cluster are determined by the distribution of the electrons relative to the amplitudes of the betatron and synchrotron oscillations. The existing theories describe the variation of the amplitudes of these oscillations during the acceleration process. The theory predicts the presence of radiation damping of the oscillations, as demonstrated first by Kolomenskii and Lebedev,¹ and also the possibility of excitation of oscillations under the influence of quantum fluctuations of the electron radiation, first pointed out by Sokolov and Ternov.²

It should be noted that to date there have been practically no experimental investigations devoted to a verification of the existing theories. The only known experimental work was performed by Sands,³ who investigated the quantum excitation of synchrotron oscillations. The present investigation was undertaken to check the basic premises of the existing theories. To investigate the quantum excitation and radiation damping of oscillations it is necessary to have on hand a cyclic electron accelerator with sufficiently high maximum energy and a long electron acceleration time. Both requirements are well satisfied by the recently constructed S-60 synchrotron of the P. N. Lebedev Physics Institute of the U.S.S.R. Academy of Sciences.⁴

This "race track" synchrotron, with four straight sections, can accelerate electrons to 660 Mev in 0.6 sec. The radius of the electron equi-

librium orbit is $R_s = 198$ cm, the fall-off exponent of the magnetic field is $n = 0.655$. The synchrotron has two resonators. The first operates as the electrons are accelerated to approximately 200 Mev, and the second—from the energy at which the first resonator is switched off to maximum. The instant of the transition from the first resonator to the second, called "interception," lies in the interval $t = 0.12 - 0.16$ sec, depending on the operating conditions of the accelerator (the time is reckoned from the instant of injection). The accelerating cycles are repeated every six seconds.

The investigation was carried out by taking high-speed motion-picture photographs of the glow of the electron cluster accelerated in the synchrotron. It should be noted that photography of the glow of the electron cluster was used earlier,^{5,6} but without photometric processing of the resultant photographs.

The apparatus used in this investigation is illustrated in Fig. 1. A mirror placed inside the vacuum chamber of the accelerator brought the electrons radiated from a segment of the orbit approximately 40 mm long out through a window in the flange of the radial tube. A lens located outside the accelerator chamber produced an intermediate image of the cluster, which was photographed with the high-speed motion-picture camera. An SKS-1 motion picture camera was used, capable of operating up to 4500 frames per second. The pictures were taken at 500 frames per second. A neon bulb fed by a 250 or 500 cps ZG-10 audio generator was used to produce the time markers on the film. A reticle graduated in millimeters was placed in

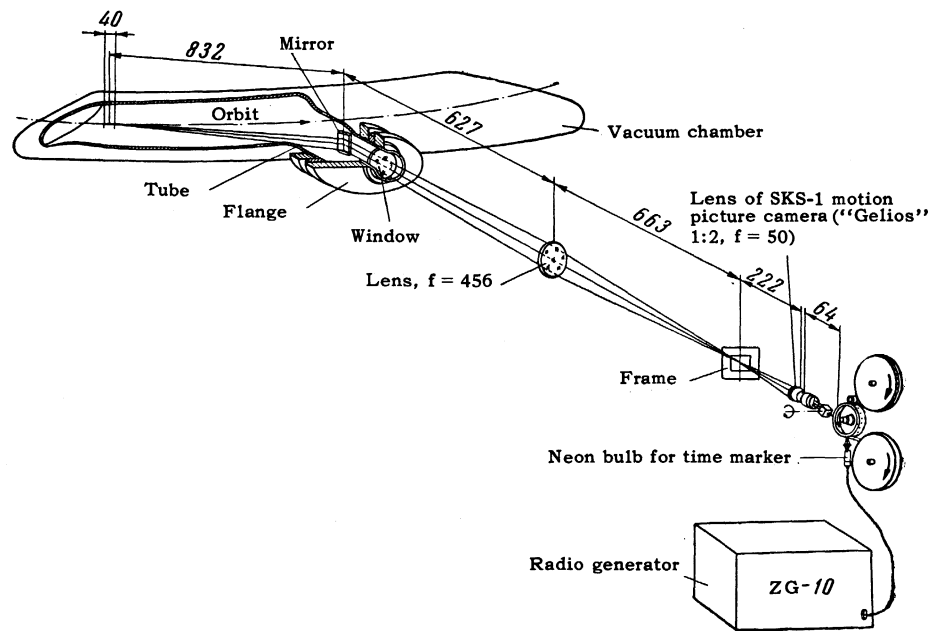


FIG. 1. Optical system of the apparatus.

the plane of the intermediate image produced by the lens, to measure the displacement of the picture of the cluster. The magnification of the optical system was 0.132. Standard MZ-2 16-mm film was used, rated 45 GOST sensitivity units. The number of electrons in the cluster, determined during the photography with a special electronic circuit, was approximately 10^7 .

To interpret the resultant cluster photographs, we must have the characteristic curve of the film so as to convert the photographic density into radiation intensity. To obtain the characteristic curve, a step wedge was placed in the plane of the intermediate image and photographed by the light of the electrons. In addition, the radiation spot incident on the wedge was photographed, to monitor any irregularities in the illumination of the wedge steps. All this made it possible to determine the characteristic curve of the film for the wide range of variation of density prevalent in the photography of electron clusters.

It took about 200 frames to photograph the cluster in a single acceleration cycle. Each frame is an image of the cross section of the electron cluster, averaged over the exposure time of the frame, equal to approximately 4×10^{-4} sec. The illumination of any portion of the image on the film is directly proportional to the number of electrons passing during the exposure time through a unit surface of the conjugate area in the cluster cross section. Thus, by measuring the distribution of the illumination in the image of the cluster, we find the distribution of the electrons over the coordinates in the cross section of the cluster, and are able to determine the width of this distribution.

A series of successive photographs of a cluster during one acceleration cycle is shown in Fig. 2, from which we can see the general character of variation of the form and dimensions of the cross section of the cluster. The same figures shows the experimental plots of the distribution of the radiation intensity over the width (radial direction of the accelerator) in height (direction of the synchrotron magnetic field).

The threshold of registration on the film amounts in our case to only ~ 100 Mev (photograph No. 1). The cluster is oval in section, slightly elongated in the radial direction, and the photographic density is low because the intensity of radiation is still low. With increasing energy, up to the instant of interception, the form of the cluster changes insignificantly, and the intensity increases. It can be assumed that directly prior to interception the form of the cross section of the cluster is determined only by the betatron oscillations (photograph No. 2). At the instant $t = 0.147$ interception takes place and causes a strong radial broadening of the cluster, owing to the occurrence of synchrotron oscillations of large amplitude (photograph No. 3). The reduction in the density of the cluster image directly after interception, compared with the photograph prior to interception, is explained by the fact that in practice the same amount of radiation is distributed over a greater image area. The initial cluster begins to fluctuate in this case as a whole, and this leads, owing to the averaging of the position of the cluster during the exposure time, to a typical picture in the form of a "dumbbell" (photographs 4 and 5). The thicker parts of the dumbbell correspond to the "turning points" of the

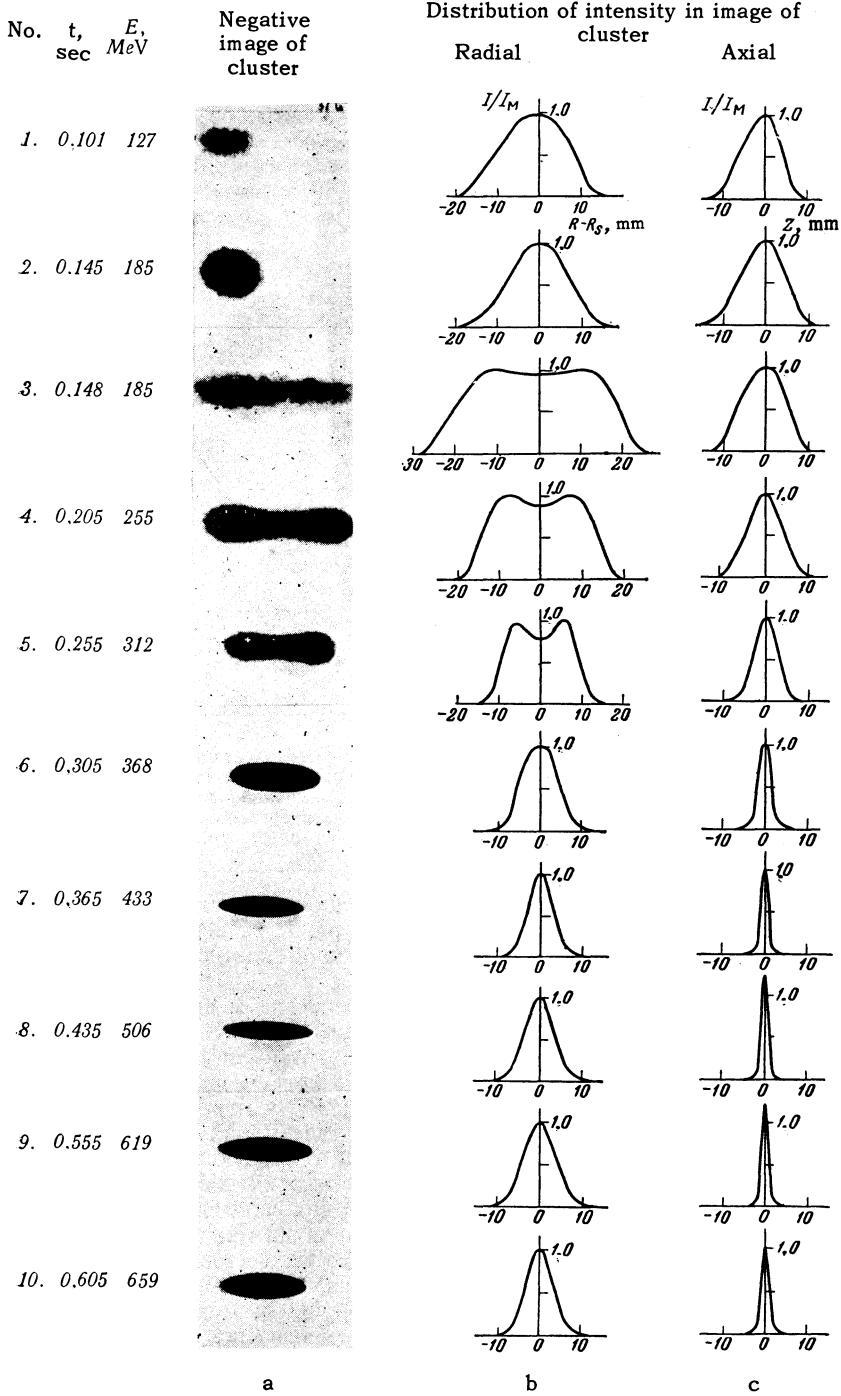


FIG. 2. Photographs of electron clusters at different instants of time in one cycle of acceleration, and corresponding distributions of radiation intensity. The ordinates represent the relative intensities.

vibrating cluster. The dimension of the cluster along the vertical direction (the z axis) remain practically unchanged during the instant of interception.

Later on, owing to the attenuation of the synchrotron and betatron oscillations, the cluster becomes compressed (picture No. 6). At the instant 0.365 sec and at an energy 433 Mev, the radial dimensions of the cluster are minimal (photograph No. 7). The cross section is similar in form at

that instant to an elongated ellipse with sharpened ends and a semi-axis ratio 1:5. The vertical dimension of the cluster reaches a minimum at the instant 0.435 when the electron energy is 506 Mev (photograph No. 8). At the end of the acceleration cycle the cluster again broadens, both radially and vertically. However, the radial broadening of the cluster reaches a limit in this case at 619 Mev and 0.555 sec (photograph No. 9), followed again by a slight radial compression of the cluster. At the

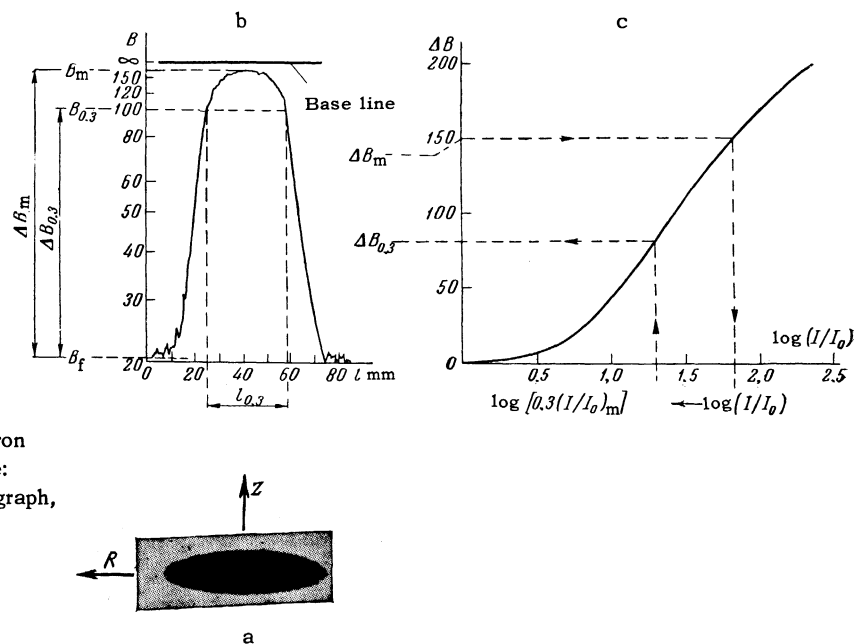


FIG. 3. Measurement of dimensions of electron clusters from the microphotograph of the picture: a – negative image of cluster, b – radial micrograph, c – characteristic curve of film.

instant when the electrons strike the target, the cluster has a form shown in photograph No. 10. The radial dimensions of the cluster become stabilized or even increase slightly apparently because of quantum build-up of the oscillations, while the stabilization and subsequent increase in the axial dimensions are still unexplained.

In order to refer the time of each frame of a given cycle to the instant of injection, the last photographed frame of the acceleration cycle was timed. On the basis of known data on the value of the electron energy in the target, the target radius, and the time necessary for the electrons to swing from the equilibrium orbit to the target, it was easy to calculate the instant of time corresponding to the start of the drift of the electron from the equilibrium orbit to the target. The error in the time correlation amounted to ± 0.01 sec. This was followed by a recalculation of the time markers produced by the neon bulb, fed from a ZG-10 generator of known frequency, so that the time corresponding to any frame of the film could be readily determined.

The electron-cluster photographs obtained were processed photometrically. An MF-4 microphotometer was used to record microphotographs of the distribution of the density in the cluster picture in two mutually perpendicular directions, corresponding to the direction of the accelerator radius R and the direction of the magnetic field z . Both directions intersected at the point of the image having the maximum photographic density. In addition, the base line, i.e., the line corresponding to in-

finite photographic density ($B = \infty$), was also recorded on the microphotograph.

Figure 3 illustrates the procedure used for the subsequent processing of the resultant microphotographs. The microphotographs for each frame chosen for processing were placed on a prepared density scale in such a way that the base lines of the microphotographs and of the scale coincided. The values of the density for the background (B_b) and for the maximum (B_m) were determined. The absolute value of the density at the maximum, $\Delta B_m = B_m - B_b$, was found.

From the characteristic curve of the photographic film we determined the logarithm of the intensity of radiation $\log(I/I_0)_m$,* corresponding to the absolute density at the maximum. To investigate the change in the radial and axial dimensions of the cluster, we measured the width of the microphotogram at a level corresponding to 0.3 of the maximum intensity, for which the logarithm of this value was determined from the formula $\log[0.3(I/I_0)_m] = \log(I/I_0)_m + \log 0.3$. The characteristic curve was then used to find the absolute value of the density for this radiation intensity level ($\Delta B_{0.3}$). Adding the value of the background, we obtained for the microphotograph the density corresponding to this level of intensity ($B_{0.3}$). The width of the microphotograph of the cluster ($l_{0.3}$) was then measured at this density level.

* I_0 is the intensity of radiation incident on a certain step of the attenuator, I is the intensity of the radiation transmitted through this step.

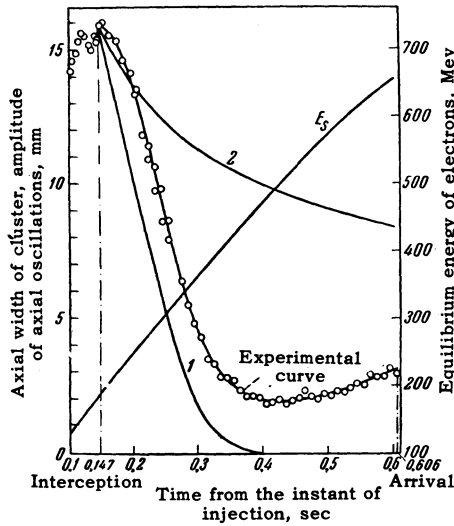


FIG. 4

Multiplying the resultant value of the width by the scale factor 0.331, we obtain the absolute value of the width of the electron distribution in the cross section of the cluster at a given level from the maximum of its distribution. Approximately 40 frames, spaced 0.01 sec apart, were processed in the series of photographs for a single acceleration cycle.

This method was used to process four frames with different electron acceleration cycles. Not one of the films enabled us to process completely the acceleration cycle, since the range of density variation from the start of acceleration until the electrons dropped on the target was so large, that it was impossible to carry out reliable photographic measurements on all the frames of the cycle. We therefore choose two films, on which part of the frames, corresponding to acceleration time from 0.1 to 0.3 sec, was reliably measured, as well as two films with reliably measured frames corresponding to the time from 0.25 to 0.6 sec.

The resultant experimental data on the variations of the axial and radial widths of the cluster at the 0.3 level for the two films, and their comparison with the theoretical variation of the summary oscillation amplitudes, are shown in Figs. 4 and 5 respectively. The choice of the width at the 0.3 level for the comparison with theory is dictated by the fact that in the photometry this width was measured most reliably. The plots for the widths at the levels corresponding to intensity values amounting to 0.2, 0.4, 0.5, and 0.6 of maximum, duplicate almost exactly the course of the given experimental curves.

In plotting the theoretical variation of the axial amplitude of the oscillations, we chose as the initial amplitude half the width of the cluster at the

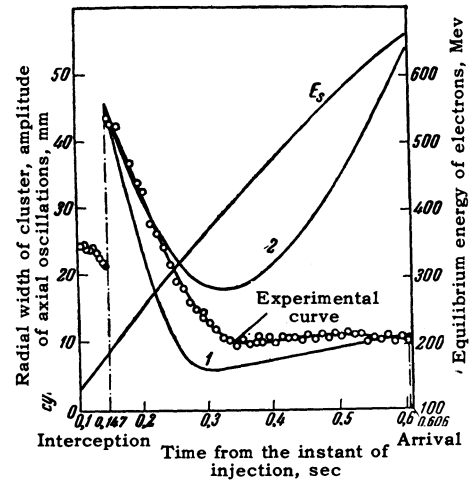


FIG. 5

instant of interception, equal to 16 mm. The initial amplitudes of the radial betatron and synchrotron oscillations were determined in the following fashion. As follows from the measurements, the radial width of the cluster prior to interception amounts to 21 mm and, apparently, is due only to betatron oscillations. At the instant of interception, the radial dimensions of the cluster increase sharply and its width becomes equal to 45.4 mm, owing to the occurrence of synchrotron oscillations. We therefore took for the initial amplitude of the radial betatron oscillations half the width of the cluster prior to interception, equal to 21 mm, and for the initial amplitude of the radial synchrotron oscillations we took half the value of the differences of the widths before and after interception, amounting to 24.4 mm. To calculate the amplitudes we make use of the Kolomenskii and Lebedev formulas⁷ in which account is taken of the radiation damping of the oscillations. The amplitude of the axial oscillations can be written here as

$$a_z = \left[a_{z_0}^2 \frac{E_{s_0}}{E_s} \exp \left(- \int_{t_0}^t \frac{W_s}{E_s} dt' \right) + \frac{13}{24 \sqrt{3}} \frac{r_0 \Lambda c}{R_s n \gamma} \int_0^t \exp \left(- \int_{t''}^t \frac{W_s}{E_s} dt' \right) \gamma^4 dt'' \right]^{1/2}, \quad (1)$$

and the summary amplitude of the radial oscillations can be written

$$a_r = \left\{ \left[a_{r_0} \left(\frac{E_{s_0}}{E_s} \right)^{1/2} \exp \left(- \frac{1}{2} \frac{n}{1-n} \int_{t_0}^t \frac{W_s}{E_s} dt' \right) + a_{r_{s_0}} \left(\frac{V}{V_0} \right)^{1/4} \times \left(\frac{E_{s_0}}{E_s} \right)^{1/4} \exp \left(- \frac{1}{2} \frac{3-4n}{1-n} \int_{t_0}^t \frac{W_s}{E_s} dt' \right) \right]^2 \frac{55}{24 \sqrt{3}} \frac{r_0 \Lambda c}{R_s (1-n)^2 \gamma} \times \int_0^t \exp \left(- \frac{n}{1-n} \int_{t''}^t \frac{W_s}{E_s} dt' \right) \gamma^8 dt'' \frac{55}{24 \sqrt{3}} \frac{r_0 \Lambda c V^{0.5}}{R_s (1-n)^2 \gamma^{1.5}} \times \int_0^t \exp \left(- \frac{3-4n}{1-n} \int_{t''}^t \frac{W_s}{E_s} dt' \right) \gamma^{6.5} V^{-0.5} dt'' \right\}^{1/2}. \quad (2)$$

The theoretical curves plotted from these formulas are denoted on both figures by the number 1. The theoretical curves, based on the Sokolov formulas in which radiation damping is not taken into account, are denoted on the same graphs by the number 2. According to theory⁸ and the law assumed for the addition of the oscillation amplitudes, the formulas for the amplitudes will have the following form: for axial oscillations

$$a_z = \left[a_{z0}^2 \frac{E_{s0}}{E_s} + \frac{13}{24\sqrt{3}} \frac{r_0 \Lambda c}{R_s n \gamma} \int_0^t \gamma^4 dt' \right]^{1/2}, \quad (3)$$

and for radial oscillations

$$a_r = \left\{ \left[a_{rb0} \frac{E_{s0}}{E_s} + a_{rs0} \left(\frac{V}{V_0} \right)^{1/4} \left(\frac{E_{s0}}{E_s} \right)^{3/4} \right. \right. \\ \times \exp \left(- \frac{13-4n}{2(1-n)} \int_{t_0}^t \frac{W_s}{E_s} dt' \right) \left. \left. + \frac{55}{24\sqrt{3}} \frac{r_0 \Lambda c}{R_s (1-n)^2 \gamma} \int_0^t \gamma^6 dt' \right] \right\}^{1/2}. \quad (4)$$

In all these formulas, a_z , a_{rb} , and a_{rs} are the amplitudes of the axial betatron, radial betatron, and radial synchrotron oscillations, respectively, E_s is the equilibrium energy of the electron, W_s is the power of the radiation emitted by the electron, r_0 is the classical electron radius, Λ is the Compton length, R_s is the radius of the equilibrium orbit, n is the exponent of the fall-off of the magnetic field, γ is the ratio of the total energy of the electron to its rest energy, and V is the high frequency voltage on the resonator. The subscript zero denotes that the corresponding quantities are taken at the instant of time t_0 . In our case $t_0 = 0.147$ sec. In addition, both plots show the build-up of the energy of the accelerated electrons, E_s .

Analyzing the experimental curves and comparing them with the theoretical ones, we can draw the following conclusions: 1) the theory that takes radiative damping into account, first developed by Kolomenskii and Lebedev,¹ gives sufficiently good albeit incomplete agreement with experiment; 2) in the energy region above 400 Mev, considerable radial oscillations are excited in the S-60 synchrotron of the Academy of Sciences Physics Institute by quantum oscillations, as first predicted by Sokolov and Ternov² and as developed in the macroatom theory of the same authors and Ivanenko³; 3) undamped axial oscillations exist, the presence of which does not follow from the theory; 4) in the energy region above 550 Mev a certain increase in the axial dimensions and a

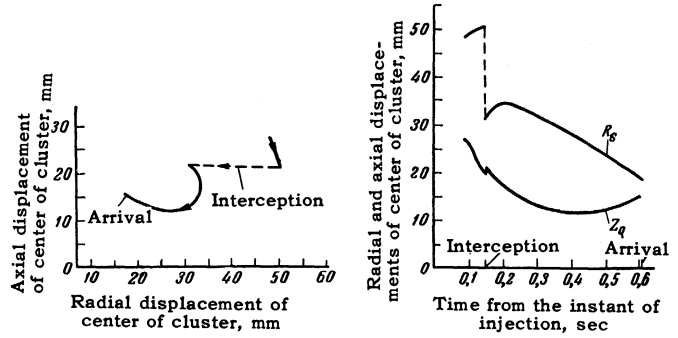


FIG. 6

small decrease in the radial dimensions of the cluster are observed in the same synchrotron, which also cannot be explained theoretically.

In the study of the variation of the axial and radial widths of the cluster at different levels away from maximum, it was observed that from the time of interception to the instant 0.32 sec ($E_s = 380$ Mev) the central part of the cluster (corresponding to the level 0.6 of maximum) is compressed more rapidly than the peripheral parts, and then the widths change at approximately the same rate. The experimental plots show also that in the time interval from the interception ($t = 0.147$ sec) to $t = 0.3$ sec, i.e., in the portion where the cluster is intensely compressed, the speed of the radial compression is approximately twice the speed of the axial compression.

By measuring the position of the center of the image of the cluster of glowing electrons relative to the edges of the image of the frame (see Fig. 1) it was possible to trace the motion of the center of the cluster in the (R, z) plane, where R is the direction of the accelerator radius and z is the direction of the magnetic field. The results of the measurements are shown in Fig. 6, from which it is seen that the cluster experiences a considerable displacement in the chamber, and that at the instant of interception a sharp change takes place in the position of the center of the cluster. These displacements are evidently due to a change in the value of the equilibrium radius and a displacement of the null z plane. The point of reference was chosen on this figure arbitrarily. The total displacement of the entire beam amounts to approximately 30 mm in the radial direction and 20 mm in the vertical direction. All these measurements pertain to a definite point of observation of the cluster in one of the quadrants of the accelerator magnet.

Thus, the optical method of observing the cluster, employed in the present work, makes it possible not only to study the change in the dimen-

sions of the cluster during the acceleration process, but also to investigate the motion of an electron beam over the cross section of the accelerator chamber.

In conclusion, the authors consider it their duty to express their gratitude to Professor M. S. Rabinovich, Professor V. A. Petukhov, and V. E. Pisarev for graciously enabling us to carry out the experiment on the S-60 synchrotron, and also to the staff members of the Physics Institute Laboratory, Yu. N. Metal'nikov, L. V. Eremin, K. N. Shorin, and E. M. Gagin for help in carrying out the experiments. The authors are also grateful to Professor A. A. Kolomenskii, Professor D. D. Ivanenko, Professor A. A. Sokolov, I. M. Ternov, A. N. Lebedev, and I. S. Danilkin for help in comparing the experiment with theory and for a discussion of the results obtained.

¹A. A. Kolomenskii and A. N. Lebedev, Dokl. Akad. Nauk SSSR 106, 807 (1956), Soviet Phys.-Doklady 1, 100 (1956).

²A. A. Sokolov and I. M. Ternov, JETP 25, 698 (1953).

³M. Sands, Nuovo cimento 15, 599 (1960).

⁴Атомная энергия (Atomic Energy) No 9, 154 (1960).

⁵Elder, Langmuir, and Pollock, Phys. Rev. 74, 52 (1948).

⁶Korolev, Akimov, Markov, and Kulikov, Тр. X Всесоюзного совещания по спектроскопии (Transactions, Tenth All-Union Conference on Spectroscopy), v. 2, L'vov 1958, p. 24.

⁷A. A. Kolomenskii and A. N. Lebedev, Ускорители элементарных частиц (Accelerators for Elementary Particles), Fourth Appendix to Journal "Atomic Energy" for 1957, p. 31.

⁸A. A. Sokolov, Введение в квантовую электродинамику (Introduction to Quantum Electrodynamics), Fizmatizdat, 1958, Sec. 28.

⁹Sokolov, Ivanenko, and Ternov, Doklady Akad. Nauk SSSR 111, 334 (1956), Soviet Phys.-Doklady 1, 658 (1957).